

# Structure-borne Sound Power Characterisation from Single and Multiple Contact Sources at Low Frequencies using Heavyweight Reception Plates

Steffi Reinhold<sup>1,2</sup>, Carl Hopkins<sup>1</sup>, Berndt Zeitler<sup>2</sup>

<sup>1</sup> Acoustics Research Unit, School of Architecture, University of Liverpool, Liverpool L69 7ZN,  
E-Mail: [steffi.reinhold@liverpool.ac.uk](mailto:steffi.reinhold@liverpool.ac.uk) and [carl.hopkins@liverpool.ac.uk](mailto:carl.hopkins@liverpool.ac.uk)

<sup>2</sup> University of Applied Sciences Stuttgart, 70174 Stuttgart, E-Mail: [berndt.zeitler@hft-stuttgart.de](mailto:berndt.zeitler@hft-stuttgart.de)

## Introduction

Structure-borne sound generated by vibrating machinery in buildings is transmitted to supporting and surrounding walls and floors before being radiated as sound pressure into other rooms. The reception plate method EN 15657 [1] can be used to estimate the structure-borne sound power of a source by using an isolated plate [2]. The source characterisation allows the prediction of radiated sound pressure levels from structures as specified in EN 12354-5 [3]. In heavyweight buildings this approach cannot always be used because there are significant errors with connected walls and floors where the response is affected by energy returning from other parts of the structure [4].

The aim of this paper is to use a validated FEM model of a heavyweight reception plate to compare the direct injected power with the reception plate power for single contact sources of randomly distributed positions. The vibrational behaviour of different harmonic point force excitations on the validated FEM model of a reception plate is compared with laboratory measurements on a reception plate. An approach is proposed to reduce measurement errors and measurement positions by using an alternative sampling strategy with an empirical weighting factor when the reception plate power is calculated. In most practical applications, building machinery has more than one contact point; hence this paper assesses the effects of multiple contact sources (e.g. white goods) attached to different positions on the FEM reception plate.

## Heavyweight reception plate test rig

The heavyweight reception plate test rig at the University of Applied Sciences in Stuttgart consists of three mutually perpendicular, independent concrete plates. The area of the plates ranges from 5.34m<sup>2</sup> to 6.85m<sup>2</sup>. Each plate is resiliently supported using viscoelastic material around the boundaries to increase their damping. Only the horizontal reception plate is studied in this paper.

## Simulation of reception plate using finite elements

In ABAQUS the linear dynamic analysis as direct frequency response solution is used to model the *in vacuo* situation (i.e. no radiation coupling). The concrete plate is created using thin triangular facet shell elements. The dimensions of elements are  $< \lambda_B/8$  over the frequency range from 20Hz to 2kHz. Resilient supports around the edges are included as spring-dashpot elements with grounded connections to the concrete plate. The properties of the resilient material were investigated in previous work [1,5,6]. The horizontal FEM reception plate has been successfully validated against measurements as described in [6,7].

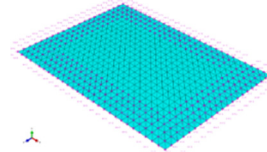


Figure 1: FEM model of horizontal reception plate.

## Characterisation of structure-borne sound power input

The reception plate method [1] is used to quantify the structure-borne sound power of sources under steady-state operating conditions with any number of contact points and geometry in the laboratory when the plate is energized into bending vibration only. The total structure-borne sound power of the vibrating source is equal to the generated plate power and is given by:

$$W_{\text{rec}} = \omega m \eta \bar{v}^2 \quad (1)$$

where  $\omega$  is the angular frequency,  $m$  is the mass,  $\eta$  is the total loss factor of the plate and  $\bar{v}^2$  is the spatial-average mean-square velocity of the plate.

For single contact sources with only perpendicular vibration forces, the active part of the complex input power directly injected into the receiver is given by:

$$W_{\text{inj}} = \frac{1}{2} \text{Re} \left[ \underline{F}^* \underline{v} \right] \quad (2)$$

where  $\underline{F}^*$  is the complex conjugate of the force and  $\underline{v}$  is the complex velocity at the driving-point.

For sources attached to the receiver with  $N$  contact points, driving with only perpendicular vibration forces, the structure-borne sound power becomes:

$$\begin{aligned} W_{\text{inj}} &= \frac{1}{2} \text{Re} \left[ \underline{F}^{\text{H}} \underline{v} \right] = \frac{1}{2} \text{Re} \left[ \underline{F}^{\text{H}} Y \underline{F} \right] \\ &= \frac{1}{2} \text{Re} \left[ \underline{\Psi}^{\text{H}} \Lambda \underline{\Psi} \right] = \frac{1}{2} \sum_{n=1}^N |\underline{\Psi}_n|^2 \lambda_n \end{aligned} \quad (3)$$

where  $\underline{F}$  and  $\underline{v}$  are complex vectors at the driving-points,  $Y$  is the real symmetric mobility matrix of the receiver and the superscript H denotes the conjugate transpose value. Using orthogonal transformation the term  $\underline{F}^{\text{H}} Y \underline{F}$  can be re-written into  $\underline{\Psi}^{\text{H}} \Lambda \underline{\Psi}$  where  $\Lambda$  is the real and non-negative diagonal matrix of eigenvalues  $\lambda_n$  of  $Y$  and  $\underline{\Psi}$  is the equivalent complex force vector [8,9]. The direct injected power (Eqs.

(2) and (3)) are used to validate the reception plate power (Eq. (1)).

### Single contact structure-borne sound sources

#### Numerical analysis using FEM

Figure 2 allows comparison of the direct injected power and the reception plate power. The latter is determined with a fine regular grid (spacing 0.05m) using all 2337 sampling positions over the plate surface. Five randomly distributed positions are considered for the harmonic point force. Close agreement ( $\pm 1\text{dB}$ ) is achieved from 20Hz to 2kHz. Whilst there are no bending modes predicted in the 63Hz and 80Hz bands, there are highly damped modes in adjacent bands which may be beneficial in reducing the error. The results also show close agreement in the 20Hz and 25Hz bands where only whole body modes occur.

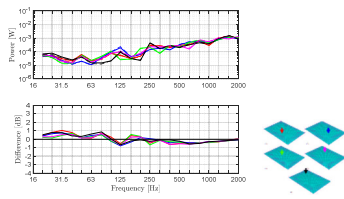


**Figure 2:** Direct injected power – solid lines, reception plate power – dashed lines (upper graph); direct injected power minus reception plate power (lower graph).

#### Comparison of numerical and experimental results

To compare the spatial variation in velocity levels from FEM with measurements, a regular grid with 0.1m spacing (total of 609 elements) is used for the FEM model of the plate. The excitation signal is broadband noise for both FEM and measurements. Figure 3 shows the contour plots of velocity levels in one-third octave bands from 50Hz to 200Hz for two different point force excitation positions. Measured and simulated results show close agreement for all seven bands.

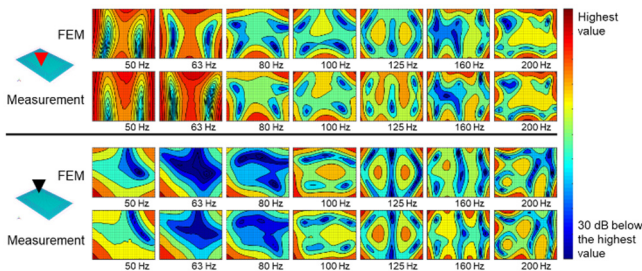


**Figure 3:** Contour plots of velocity levels from simulation and measurement: red point force excitation – central zone of the plate (above black line) and black point force excitation – close to corner of the plate (below black line).

In Figure 4 the velocity levels of the central zone ( $\geq 0.5\text{m}$  away from edges) are normalised to the direct injected power at the driving-point to facilitate comparison between FEM and measurements. This shows reasonably close agreement (within 3dB).

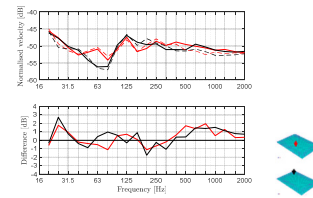


**Figure 4:** Normalised velocity levels: FEM simulation – solid lines, measurement – dashed lines (upper graph); difference of normalised velocity levels between FEM simulation and measurement (lower graph).

#### Sampling strategy proposal for reception plate method

Measurements can be time consuming and therefore it is useful to consider whether the number of positions can be minimised, while still achieving a suitably accurate estimate. A sampling strategy is developed for the spatial-average velocity to correctly estimate the reception plate power using positions over the entire plate surface (particularly at low frequencies). Contour plots in Figure 3 indicate that velocity levels at corners tend to be larger than the velocity levels in the central zone. For field measurements of airborne sound insulation between rooms similar issues were identified at low frequencies [10]. A similar approach is used here to estimate the reception plate power by introducing an empirical weighting factor  $X$  that combines the measured velocities from all four corners and the central zone ( $\geq 0.5\text{m}$  away from edges) of the reception plate. Using this weighting factor  $X$ , the combined spatial-average velocity is defined as:

$$L_v = 10 \lg \left[ \frac{X \cdot 10^{L_{\text{CentralZone}}/10} + 10^{L_{\text{Corner}}/10}}{X + 1} \right] \quad (4)$$

The proposed empirical weighting factor  $X$  (see Figure 5), is 1 at frequencies up to 40Hz. At 50Hz,  $X$  is raised to 2 and then increases by a factor of 3 per doubling of frequency in order that the corners have less of an effect on the average velocity.

Applying this weighting leads to reasonable agreement ( $\pm 3\text{dB}$ ) between the direct injected power and the reception plate power up to 125Hz where the mode count is low (see Figure 6). Above 125Hz the agreement improves to  $\pm 1.5\text{dB}$  as the mode counts increase with increasing frequency.

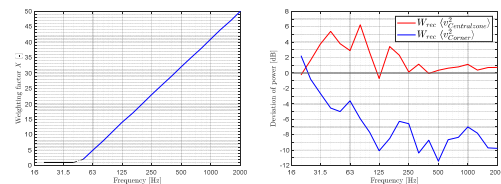


**Figure 5:** (Left) Weighting factor  $X$  for reception plate power. (Right) Direct injected power minus reception plate power for central zone and corner positions.

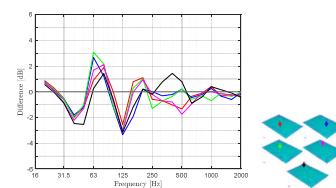


**Figure 6:** Direct injected power minus reception plate power using weighting factor  $X$ .

## Multiple contact structure-borne sound sources Numerical simulation of experiments with FEM

Most machinery are multiple contact sources such as white goods (e.g. washing machines) with four contacts in a 60 x 60cm square. These are numerically investigated using the validated FEM reception plate model. The reception plate power is estimated using all elements for the spatial-average velocity and the excitation signal is applied as a uniform harmonic point force with in- or random-phases between the four contact points.

The multiple contact source is initially aligned parallel to the reception plate boundaries assuming in-phase difference between the forces at the contact points. There is close agreement (within 1dB) between the direct injected power and the reception plate power for excitation positions that have at least two positions close to corners or edges as shown in Figure 7. For sources that are placed in the central zone of the plate a difference up to 3dB occurs at 500Hz because at this frequency the lateral distance between the contact points equates nearly one-half of the bending wavelength of the reception plate. In the contour plots it can be seen that underneath the machine the highest velocity levels occur at 500Hz. This indicates that sources with four in-phase contacts force the plate to have a high response by forcing a half-wavelength response between the contact points. These results lead to an overestimation of the reception plate power at this frequency. For sources that are close to corners/edges this issue does not arise because the driving-point mobility of the contacts are sufficiently different in terms of the magnitude and phase, and the modes have usually a high response near corners and edges. The problem still occurs when excluding all elements within a 0.1m radius of each contacts (see Figure 8). For central zone positions the overestimation of the reception plate power can only be avoided by excluding all elements underneath the source and up to 0.1m away from all contact points although the reception plate power is underestimated for sources near corners/edges up to 500Hz.

When the source is aligned at an angle to the plate edges (see Figure 9), similar results occur with in-phase assumption. It is noted that the difference between both powers improves slightly compared to sources that are aligned parallel to the plate perimeter (particularly at 500Hz).

In Figure 10 the multiple contact sources are aligned parallel to the plate boundaries but the forces use the random-phase assumption. Comparison of both powers show close agreement ( $\pm 1$ dB) for sources placed near corners/edges as well as in the central zone of the plate when all elements are considered for the estimation of the reception plate power. By excluding elements underneath the machine and up to 0.1m away from all excitation positions there is still close agreement ( $\pm 1$ dB) for sources in the plate's central zone. However, for sources near corners/edges the difference between the direct injected power and the reception plate power increases up to 2dB at low frequencies.

For the structure-borne sound power characterisation of square multiple contact sources a few approaches could be specified in measurement standards to avoid errors relating to

the estimation of the reception plate power. The problems identified here indicate an overestimation or underestimation of the reception plate power which is dependent on the source location on the plate and the phase difference between the forces at the contact points. This particularly occurs in the low-frequency range or at frequencies where the distance between the contacts correspond to one-half of the bending wavelength of the plate. Therefore, in absence of detailed information about the phase difference between the contact forces, errors could be avoided by placing these sources in the central zone instead of near corners/edges and excluding all elements underneath the machine and up to 0.1m away from all four contact positions.

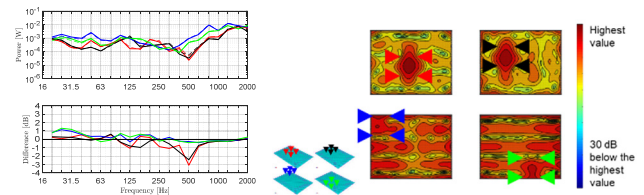


**Figure 7:** White goods aligned parallel to plate edges assuming in-phase forces: (Left) Direct injected power – solid lines, reception plate power with all elements – dashed lines (upper graph); direct injected power minus reception plate power (lower graph). (Right) Contour plots of velocity levels over the plate surface at 500 Hz.

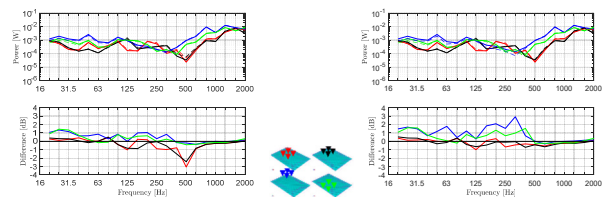


**Figure 8:** White goods aligned parallel to plate edges assuming in-phase forces: Direct injected power – solid lines, reception plate power with all elements – dashed lines (upper graph); direct injected power minus reception plate power (lower graph). (Left) Excluding elements within 0.1m radius of each contact. (Right) Excluding all elements underneath the machine and up to 0.1m away from all four contacts.

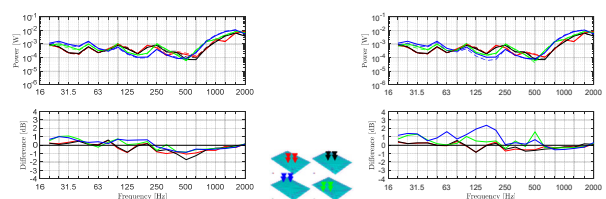


**Figure 9:** White goods aligned at an angle to plate edges assuming in-phase forces: Direct injected power – solid lines, reception plate power with all elements – dashed lines (upper graph); direct injected power minus reception plate power (lower graph). (Left) All elements. (Right) Excluding all elements underneath the machine and up to 0.1m away from all four contact points.

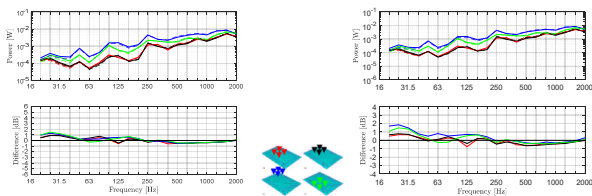


**Figure 10:** White goods aligned parallel to plate edges assuming random-phase forces: Direct injected power – solid lines, reception plate power with all elements – dashed lines (upper graph); direct injected power minus reception plate power (lower graph). (Left) All elements. (Right) Excluding all elements underneath the machine and up to 0.1m away from all four contact points.

### Sampling strategy estimation for reception plate method

The proposed empirical weighting is also used for multiple contact sources when the reception plate power is obtained by excluding all elements underneath the source and up to 0.1m away from all four contacts. For sources in the central zone there is reasonable good agreement ( $\pm 4$ dB) for in-phase forces which decreases to  $\pm 3$ dB with random-phase forces. When the source is placed near corners/edges reasonable agreement ( $\pm 4$ dB) is achieved for both in- and random-phase forces. Note for sources near corners/edges the reception plate power still tends to be underestimated.

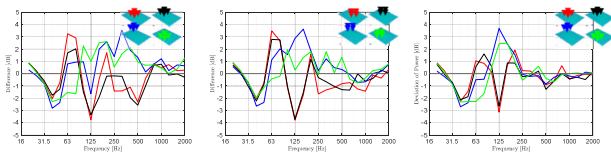


**Figure 11:** White goods: Direct injected power minus reception plate power when using the weighting factor  $X$  to determine reception plate power. (Left) In-phase forces and parallel to plate edges. (Middle) In-phase forces and angle to plate edges. (Right) Random-phase forces and parallel to plate edges.

### Conclusions

The effects of single and multiple contact sources have been investigated using a validated FEM model of a heavyweight reception plate. For single contact sources the lowest differences between the direct injected power and reception plate power are achieved when the spatial-average velocity is determined using a regular grid over the entire plate surface. The validity of the FEM model is confirmed by comparison with experimental data. This confirms that the analytical model can be used to assess a sampling strategy for laboratory experiments. A sampling strategy using an empirical weighting factor is proposed based on the spatial-average velocity at the four corners and the central zone of the FEM reception plate. For numerical experiments of square multiple contact sources such as white goods it is essential to have detailed information about the phase difference between the forces at the contact points. When the phase difference is not known the source should be placed in the central zone of the plate by excluding all elements underneath the machine and up to 0.1m away from all contact points.

Future work will aim to minimise the number of measurement positions in the central zone of the plate and to estimate Fast time-weighted levels from short equivalent continuous levels.

### References

- [1] EN 15657: Acoustics properties of building elements and of buildings – Laboratory measurement of structure borne sound from building service equipment for all installation conditions, 2017.
- [2] M. M. Späh, B. M. Gibbs. Reception plate method for characterisation of structure-borne sound sources in buildings: Assumptions and application, *Applied Acoustics* 2009, 70, 361-368.
- [3] EN 12354-5: Building acoustics – Estimation of acoustic performance of building from the performance of Experimental work elements – Part 5: Sound levels due to service equipment, 2009.
- [4] C. Hopkins, M. Robinson. Using transient and steady-state SEA to assess potential errors in the measurement of structure-borne power input from machinery on coupled reception plates, *Applied Acoustics* 2014, 79, 35-41.
- [5] C. Hopkins. Sound insulation, Butterworth-Heinemann, 2007, ISBN 978-0-7506-6526-1.
- [6] S. Reinhold, C. Hopkins, B. Zeitler. Finite element simulation of a laboratory reception plate for structure-borne sound power measurements, *Proceedings of the 45<sup>th</sup> International Congress and Exposition of Noise Control Engineering* 2016, 1-9, Hamburg.
- [7] S. Reinhold, C. Hopkins, B. Zeitler. Numerical simulation of a laboratory reception plate using finite elements, *Proceedings of the German Annual Conference on Acoustics (DAGA)* 2017, 6-9, Kiel.
- [8] L. Ji, B. R. Mace, R. J. Pennington. A power mode approach to estimating vibrational power transmitted by multiple sources, *Journal of Sound and Vibration* 2003, 265, 387-399.
- [9] S. Jianxin, A. T. Moorhouse, B. M. Gibbs. Towards a practical characterisation for structure-borne sound sources based on mobility techniques, *Journal of Sound and Vibration* 1995, 185(4), 737-741.
- [10] C. Hopkins, P. Turner. Field measurements of airborne sound insulation between rooms with non-diffuse sound fields at low frequencies, *Applied Acoustics* 2005, 66, 1339-1382.